Biosensors and Bioelectronics 157 (2020) 112161

Contents lists available at ScienceDirect

Biosensors and Bioelectronics

journal homepage: http://www.elsevier.com/locate/bios

Norepinephrine as new functional monomer for molecular imprinting: An applicative study for the optical sensing of cardiac biomarkers

V. Baldoneschi, P. Palladino, M. Banchini, M. Minunni, S. Scarano *

Department of Chemistry "Ugo Schiff", University of Florence, 50019, Sesto Fiorentino (FI), Italy

ARTICLE INFO

Keywords:
Polynorepinephrine
Surface plasmon resonance
Molecular imprinting
Functional monomer
Troponin
Epitope imprinted biosensors

ABSTRACT

The continuous research for alternatives to antibody-based detection drove, in the last decades, the development of numerous strategies. Molecularly imprinted polymers (MIPs) emerged thanks to the low-cost and long-term stability features, where the choice of natural functional monomer(s) represents the key step for efficient imprinting of biomolecules. The chemical structure of dopamine (DA), one of the most used natural functional monomers, provided the inspiration for this work. We wondered why norepinephrine (NE) that differs from dopamine only for an additional hydroxyl group was not investigated at all in biosensing applications. In fact, there is only one paper exploiting polynorepinephrine (PNE) in molecular recognition applications, taking advantage of molecular imprinting, but not for biosensing purposes. In contrast, hundreds of papers describe polydopamine-based sensors. Therefore, we firstly investigated how the additional hydroxyl group of NE could affect the properties of the resulting polymer, and how these properties could be exploited for biosensing applications. The results highlighted the reduced non-specific adsorption of proteins onto PNE with respect to dopamine polymer. Furthermore, as a case study, we successfully developed a PNE-based imprinted biosensor for the early detection of Troponin I, a crucial biomarker for heart failure, by coupling the MIP biosensor with surface plasmon resonance (SPR) detection. The results indicate the feasible use of imprinted PNE as synthetic receptor for biomolecules, opening new perspectives for this biopolymer, so far not considered, and encouraging further investigations on its potential application in biosensing.

1. Introduction

The use of biomimetic receptors for the development of innovative and antibody-free analytical platforms, including affinity sensing, represents an important challenge in bioanalytical chemistry. In this field, MIPs emerged as particularly useful tools for biosensing applications (Uzun and Turner, 2016; Zaidi, 2017) thanks to the low-cost and long-term stability features, where the choice of natural functional monomer(s) represents the key step for efficient imprinting of biomolecules. Dopamine encountered an impressive success as functional monomer for molecular imprinting of polydopamine (PDA) (Palladino et al., 2019, 2018; Zaidi, 2019; Zhang et al., 2018) while NE, differing from DA only for an additional hydroxyl group (Fig. 1a), has not yet been exploited for MIP-based biosensing.

In the last ten years PNE has been investigated in various applications, including modification of surfaces for immobilization of enzymes in nanobiocatalysis, or as coating for drug release nanosystems (Baldoneschi et al., 2020; He et al., 2019; Kang et al., 2009; Nejad et al., 2018; Yang et al., 2015). In few cases NE was exploited as template for molecular imprinting, for example in chromatographic chiral separation of neurotransmitters, and in electrochemical and quantum dots-based sensing for NE determination (Casadio et al., 2017; Huang et al., 2011; Rosy et al., 2014; Wei et al., 2014). However, to the best of our knowledge, only one paper dealing with PNE imprinting has been published. It consists in a solid phase polymer for the enantio-separation of small molecules, where NE has been polymerized in presence of the chiral templates (L-amino acids, S-(−)-ofloxacin and S-(−)-binaphthol) on the surface of magnetic nanoparticles (Chen et al., 2015).

In this framework, we recently started to investigate new outlooks of PNE in bioanalytical chemistry (unpublished results) and here we report the first example of PNE-based MIP as recognition element for affinity sensing, opening to the perspective use of other catecholamine family members in molecular imprinting.

Both these catecholamines, DA and NE, are essential

* Corresponding author.
E-mail addresses: veronica.baldoneschi@unifi.it (V. Baldoneschi), pasquale.palladino@unifi.it (P. Palladino), marco.banchini@stud.unifi.it (M. Banchini), maria.minunni@unifi.it (M. Minunni), simona.scarano@unifi.it (S. Scarano).

https://doi.org/10.1016/j.bios.2020.112161
Received 10 January 2020; Received in revised form 16 March 2020; Accepted 17 March 2020
Available online 20 March 2020
0956-5663/© 2020 Elsevier B.V. All rights reserved.

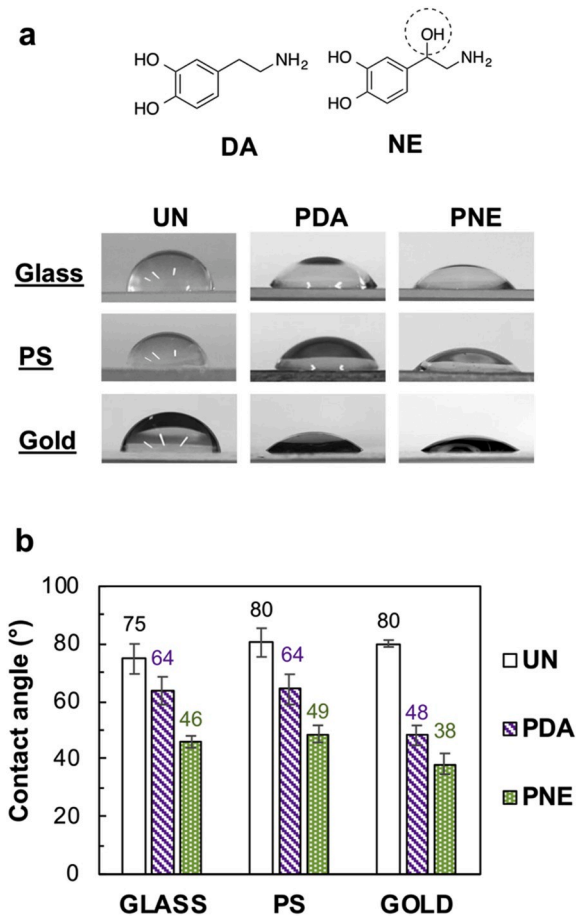

Fig. 1. (a) Chemical structure of NE and DA and representative images of water drops on untreated (UN) or treated glass, PS and gold surfaces coated with PDA or PNE. (b) Contact angle measurements reported as mean value of four replicates, determined 30 s after the drop deposition.

neurotransmitters and are able to easily self-polymerize in alkaline conditions through oxidative polymerization, by forming adherent films on various type of surfaces, such as noble metals, metal oxides, glass and synthetic polymers (Blows, 2000; Jeon and Kang, 2013; Palladino et al., 2019, 2018; Scarano et al., 2019, 2018; Zaidi, 2019).

On the other hand, two features distinguish PNE from PDA: the presence of the hydroxyl group in the benzylic position of NE (Fig. 1a) and the smoothness at the nanometer scale given by the intermediate 3,4-dihydroxybenzaldehyde norepinephrine (DHBA-NE) isolated by Hong et al. by HPLC-MS, whose structure solved by NMR spectroscopy (Hong et al., 2013; Yang et al., 2015). Therefore, the repeated hydroxyl functional groups of PNE should lead to higher hydrophilicity of the MIP surface, reducing the non-specific adsorption of proteins and favoring the selective binding of the target analyte. Furthermore, the smooth MIP surface could circumvent the limits of dopamine concerning the uncontrollable surface morphology and the formation of precipitates during the polymerization (Hong et al., 2013). In a recent work, we presented the first example of epitope-imprinted surface plasmon resonance (SPR) biosensor based on PDA for cardiac Troponin T (TnT) detection (Palladino et al., 2018), one of the preferred biomarkers in acute myocardial infarction (AMI) diagnosis. The epitope approach, wherein only short peptides belonging to the protein structure are printed, can overcome the drawbacks of the whole protein imprinting in MIPs. In particular, this choice improves the sensor selectivity by minimizing the non-specific binding; circumvents the problem of conformational changes of the template; and reduces the costs, since peptides are considerably less expensive than the full proteins (Singh et al., 2017). In the present paper, PNE is investigated for epitope-imprinting and compared to PDA performances by optical biosensing. As a case study, we report here the detection of Troponin I (TnI), *i.e.* the subunit 'I' of the troponin complex I-C-T, which is another crucial biomarker for AMI diagnosis (Wettersten and Maisel, 2015; Zahran et al., 2018). We first explored, by contact angle measurements, the enhanced hydrophilicity of PNE coated surfaces with respect to PDA, and then the resulting effects on the non-specific adsorption of proteins through SPR biosensing. Finally, the imprinting of two short TnI peptides on PNE has been performed on gold sensor chips and the sensing efficiency and selectivity of the relative optical biosensor has been investigated in buffer and in human plasma by means of SPR, a reference platform for label-free detection of macromolecular interactions (D'Agata et al., 2017; Palladino et al., 2018, 2016; 2011; Torrini et al., 2019).

2. Material and methods

2.1. Reagents

Dopamine hydrochloride, ±-norepinephrine hydrochloride, tris (hydroxymethyl)aminoethane hydrochloride (Tris-HCl), hydrochloric acid, acetic acid, human serum from human male AB plasma sterile-filtered, bovine serum albumin, glycine, sodium dodecyl sulphate (SDS) and Tween-20 were purchased from Merck (Italy). The synthetic C-terminus peptide of TnI (residues 197-210: ALSGMEGRKKKFES) and the N-terminus peptide of TnI (residues 28-40: AYATEPHAKKKSK) were identified according to the epitope-imprinting strategy (see paragraph 2.3) previously applied to TnT (Palladino et al., 2018) and then purchased from Genscript (USA). Bare gold and streptavidin coated gold sensor chips were purchased from GE Health Care (Italy). Recombinant human cardiac troponin I-C complex (TnIC) was purchased from Spectral Medical Inc (USA). Anti-human troponin I mouse monoclonal antibodies 19C7 and TPC110 clones, were purchased from Hytest (Finland) and SDIX (USA), respectively. Pierce streptavidin magnetic beads were purchased from Fisher Scientific (Italy). Biotinylated mouse monoclonal troponin I antibody (MF4 clone), anti-troponin C antibody (OTI5H3 clone), and anti-troponin C antibody conjugated to alkaline phosphatase (LS-C511913 clone) were purchased from Novus Biologicals (Italy).

2.2. Contact angle measurements

The surface wettability of three different substrates (*i.e.* glass, polystyrene and gold), with or without PNE or PDA coating, was determined by contact angle measurements. Firstly, the substrates were vertically immersed in a solution of PNE or PDA (5 g L^{-1} in 20 mM Tris-HCl pH 8.5) for 24 h at 25 °C, then they were gently washed with H_2O and dried under nitrogen flush. The image of a 10 μL drop of water was captured, after 30 s from the deposition, by a smartphone camera equipped with a macro lens (15X magnification, Evershop). The images were processed by ImageJ software using DropSnake plugin.

2.3. Analyte and template selection

The cardiac troponin complex is constituted by troponin I, T and C (TnI, TnT and TnC) and it is responsible for cardiac muscle contraction. Upon myocardial infarction troponin is released from myocytes in the blood in the following forms: a) trimeric complex I-T-C; b) free TnT, TnI and TnC; c) dimeric complex TnIC (Park et al., 2017). TnI and TnT are formally preferred as targets for cardiac injury immunoassays, considering that their isoforms are specific for skeletal or cardiac muscle (Wettersten and Maisel, 2015). However, cardiac and skeletal isoforms of TnC are equivalent, thus TnC assays would not be suitable for patients with skeletal muscle disease or trauma. Concerning TnI, the purified form is highly susceptible to proteolysis, while in the dimeric complex

TnIC, TnI is protected by TnC that interacts with the TnI central region (Katrukha et al., 1998; Morjana, 1998). Moreover, TnIC complex was found to be predominant in the blood of AMI patients, with respect to the tertiary complex I-C-T and to free TnI (Giuliani et al., 1999; Katrukha et al., 1997). Therefore, we selected TnIC as target analyte, as the monomeric form is extremely unstable and present at a lower level in the blood of AMI patients (Katrukha et al., 1998). In the template selection for the imprinting process we followed the epitope approach, which is usually applied to preserve or increase the biological recognition capability of more complex and expensive physiological molecules (Accardo et al., 2011; Palladino et al., 2018, 2012). Here the epitope approach helps to circumvent the difficulties of the whole protein imprinting, due for example to the large size and to conformational changes that can occur in non-physiological conditions (Ansari and Masoum, 2019). The TnI peptides selection was then made according to chemical composition and to structural considerations based on the X-ray crystal structure of troponin complex (PDB ID: 4Y99; 1J1E. Takeda et al., 2003). TnI is a 209 amino acids long protein consisting in five domains. The X-ray structure indicates that the region between residues 42 and 136 (*i.e.* IT arm) is characterized by two helices connected by a short linker (Katrukha, 2013). The high rigidity of this domain could represent an obstacle for the imprinting process, since the helical conformation could not be preserved by the analogous peptides in solution and during the polymerization. In addition, the central region of TnI is almost superimposable to sequence of slow and fast skeletal muscle subtypes, which could impair the specific recognition of TnI. On the contrary, the C-terminal and N-terminal regions of TnI are specific for the cardiac isotype, are flexible and rich in lysine, whose amine groups should favor the interaction of TnI peptides with catecholamine during polymerization (Palladino et al., 2018). Taking into account of these considerations, the C-terminal region 197–210 and the N-terminal region 28–40 were selected as templates for the imprinting process.

2.4. Sensor chips preparation and SPR experiments set up

Bare gold SPR chips were coated with PDA or PNE films by applying a 5 g L^{-1} solution of DA or NE respectively by drop casting, in 20 mM Tris-HCl pH 8.5, in presence (MIP) or not (NIP) of the template (1 g L^{-1}). After 5 h at 25 °C each chip surface was gently washed with acetic acid (aq. 5% v/v), 10 mM Tris-HCl pH 8.5, and H_2O. The polymer-coated sensor chips were mounted into the SPR instrumentation and conditioned at 5 μL min^{-1} at 25 °C in PBS pH 7.4 as running buffer. The measurements were conducted by injecting the analyte (20 μL) on the optical sensor surfaces (flow rate: 5 μL min^{-1}; temperature: 25 °C) on single or double flow channel mode. After each binding measurement, the surfaces were regenerated by 0.05% SDS (10 μL) and 10 mM HCl (10 μL) in water. All the SPR experiments were performed on Biacore™ X and Biacore™ X100 machines (GE Healthcare) and the data were analyzed by BIAevaluation 3.1 software.

2.5. Analyte extraction from human serum

The extraction of the target TnIC from human serum was performed through streptavidin-coated magnetic beads, functionalized with a biotinylated anti-TnI antibody. After removal of the starting supernatant by magnetic separation, the magnetic beads (0.5 mg) were washed with 1 mL of binding/wash buffer (Tris-buffered saline including 0.1% of Tween-20). A 10 mg L^{-1} solution of the TnIC antibody (clone MF4) in binding buffer was added to the beads and the mixture was incubated for 1 h at room temperature with mixing. The beads were collected and washed with wash buffer (4 × 500 μL), then the spiked sample was added to the functionalized beads and the mixture was incubated for 2 h at room temperature. The beads were washed with wash buffer (4 × 500 μL) and finally, the analyte was eluted with glycine pH 4.0 (100 μL) and neutralized with PBS pH 7.4 (400 μL).

3. Results and discussion

The polymerized PNE was evaluated in its behavior in coating chip surfaces with special attention on surface wettability, non-specific adsorption versus real matrix potential components (proteins), imprinting and MIP realization with desired specificity, eventually Troponin I, a key marker in acute myocardial infarction (AMI), analytical application of the MIP in matrices of clinical interest (serum).

3.1. Enhanced surface wettability induced by PNE

We determined the surface wettability of three different substrates (*i.e.* glass, polystyrene (PS) and gold), untreated (UN) or treated with PNE or PDA coating, by contact angle measurements, in order to evaluate the hydrophilic character induced by the growth of the two polymers on the surface. As expected, both PDA and PNE coating induced a higher wettability in all the materials with respect to the untreated surfaces (Fig. 1a). However, the treatment with PNE coating caused a larger increase of the wettability respect to PDA, resulting in a difference of 29°, 31° and 42° for glass, PS and gold, respectively, versus the uncoated samples (Fig. 1b). The presence of the hydroxyl group spread over the PNE polymeric network likely increases the hydrophilicity of the surface, with respect to PDA coatings, that do not contain the same functional groups. Such enhanced hydrophilicity of PNE could limit the hydrophobic interactions that are responsible of the non-specific binding of proteins on PDA coatings, thus favoring the specific interactions on MIP surfaces (Buchwalow et al., 2011; Kastritis and Bonvin, 2012).

3.2. Non-specific adsorption on PNE compared to PDA

Non-specific binding (NSB), caused by matrix components, is a critical parameter in SPR, as well as in generic microfluidic biosensors, since it may produce false-positive results that mask the signal of the target analyte, reducing the accuracy of the assay. The protein-adsorption capacity of PDA-coated surfaces is extensively reported in literature (Goh et al., 2018; Ku et al., 2010; Pop-Georgievski et al., 2011; Sy et al., 2018). PNE shares with PDA the same active groups, but we hypothesized that the presence of the additional hydroxyl function of NE, spread over all the polymeric network, could reduce the hydrophobic interactions between proteins and polymer that are among the causes of NSB, thanks to the higher hydrophilic character of the surface. In our experiments, PDA and PNE have been grown directly onto the gold surface of SPR sensor chips for 5 h at room temperature without any template (NIP) to assess the protein adsorption capacity, regardless of surface imprinting. The protein adsorption capacity of PNE and PDA films was tested toward three proteins of different nature: bovine serum albumin (BSA); anti TnC antibody (OTI5H3 clone) and TnIC. The first one is a protein widely used as blocking agent in immunoassays, because it readily adsorbs on foreign surfaces dominating the first stages of proteins adsorption (Peters, 1996). OTI5H3 is a representative monoclonal antibody anti-TnC, regularly used in TnI detection assays in order to ensure the capture of the dimeric complex TnIC. Finally, TnIC is considered the target analyte in our application study, as previously described, thus we were interested in evaluating possible NSB with the not imprinted polymer, to obtain information about the selectivity of the following MIP. Fig. 2 shows that BSA (1 g L^{-1}), as well as the antibody and TnIC (1 mg L^{-1}), were highly adsorbed on the PDA film, by resulting in 1.944 ± 657, 759 ± 43 and 571 ± 123 resonance units (RU) from SPR experiments, respectively on three replicates. On the contrary, the protein adsorption is strongly reduced on the PNE film, up to 87% for BSA, 93% for the antibody and 60% for TnIC, suggesting that the presence of the hydroxyl function in the polymeric network of PNE could reduce the hydrophobic interactions responsible of NSB. In addition, the experiments performed on the PNE sensor chip resulted more reproducible then those performed on the PDA film, as indicated by the lower standard deviation bars.

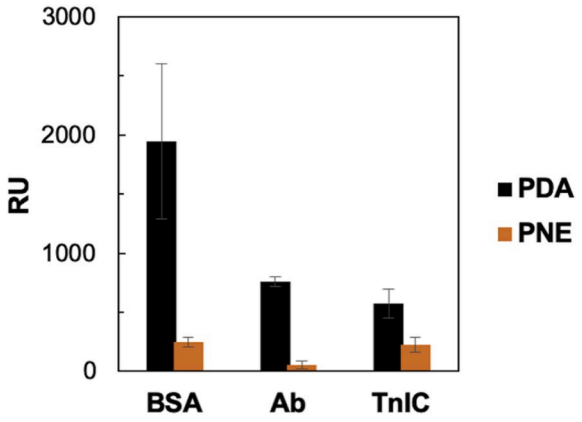

Fig. 2. Response of PDA- and PNE-based NIP biosensors at 1 g L^{-1} of BSA, 1 mg L^{-1} of anti-TnC antibody (Ab) and 1 mg L^{-1} of TnIC. The results are reported as mean value of three independent replicates for each analyte injection. Each injection was followed by a regeneration step.

3.3. PNE epitope imprinting

The C-terminal (^{197}ALSGMEGRKKKFES^{210}) and N-terminal (^{28}AYATEPHAKKKSK^{40}) peptides of TnI were separately used as template in PNE imprinting process, according to the epitope-approach (Fig. 3a) and to the structural considerations described before. In particular, the bare gold sensor chips were kept in contact with a mixture of 5 g L^{-1} NE and 1 g L^{-1} solution of C-terminal, or N-terminal, peptide in 20 mM Tris-HCl pH 8.5, for 5 h at 25 °C (step 1). After template removal with acetic acid (5% v/v) and washing with Tris-HCl pH 8.5 and H_2O (step 2), the imprinted sensor chips were tested for their binding capacity toward TnIC (step 3). Fig. 3b shows that the imprinting with the N-terminal peptide resulted in a higher SPR response, by gaining about further 100 RU with respect to the biosensor imprinted with the C-terminal of TnI. In addition, by comparing these results with the one obtained on the NIP sensor chip, the imprinting of PNE led to an improved binding capacity and to a better reproducibility, as expected, likely thanks to the selective capture of the analyte.

3.4. MIP selectivity

The selectivity of the MIP sensor chip, imprinted with the N-terminal peptide of TnI, was investigated by injecting a panel of proteins and antibodies that could lead to NSB on the sensor surface, hence leading to false-positive results in a hypothetic TnI bioassay. The following proteins were injected: a) TnT, *i.e.* the other monomer forming the troponin complex; b) human serum albumin (HSA), being the main component of human serum; c) TPC110, 19C7 and MF4, which are three mouse monoclonal anti-TnI antibodies commonly used in commercial TnI immunoassays. TnIC, TnT and HSA were injected at 20 nM concentration, while the antibodies were used at 7 nM, corresponding to 1 mg L^{-1}. As result, the MIP biosensor showed an excellent selectivity toward the target TnIC, which was the main analyte interacting with the imprinted biosensor (Fig. 4). These results make the MIP surface a promising synthetic receptor for the development of a TnI sensing assay, thanks to the compatibility with eventual interfering reagents present in the sample or in the assay kit.

3.5. Comparing MIP biosensor with an immuno-based sensor chip

The MIP sensor chip was directly compared to another SPR sensor functionalized with anti-TnI antibodies, in order to point out the advantages in the use of a low-cost polymer as an alternative to classic antibodies for biosensing applications. Some examples reporting direct comparison between antibodies and synthetic receptors are reported in

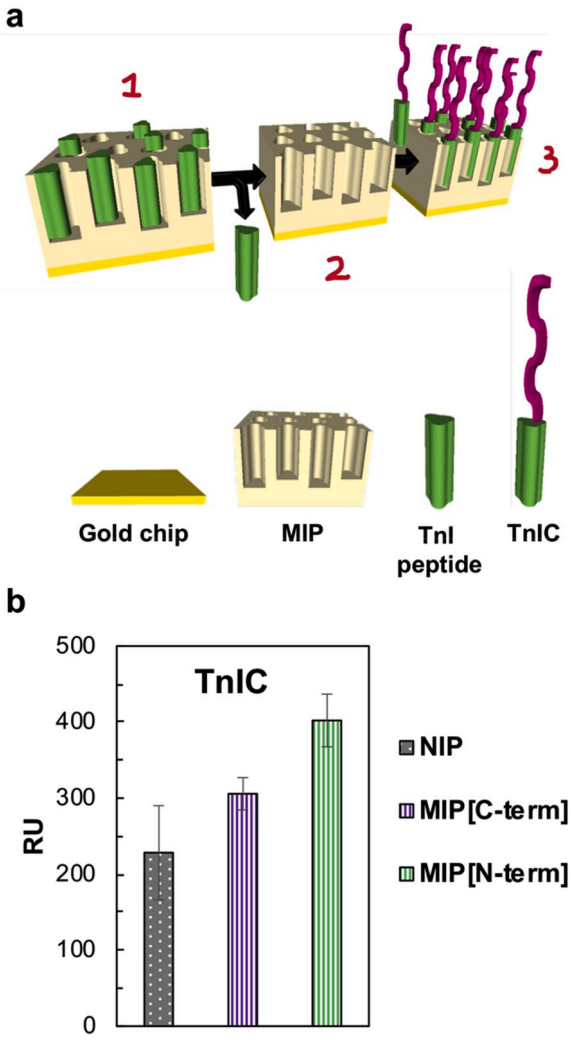

Fig. 3. (a) Scheme of the epitope imprinting strategy: the functional monomer NE was polymerized in presence of the TnI peptide (template), which was then removed, by living cavities that are able to recognize the whole protein TnIC. (b) Response of PNE-based NIP and MIP biosensors at 1 mg L^{-1} of TnIC. The results are reported as mean value of three replicates for each analyte injections. Each injection was followed by a regeneration step.

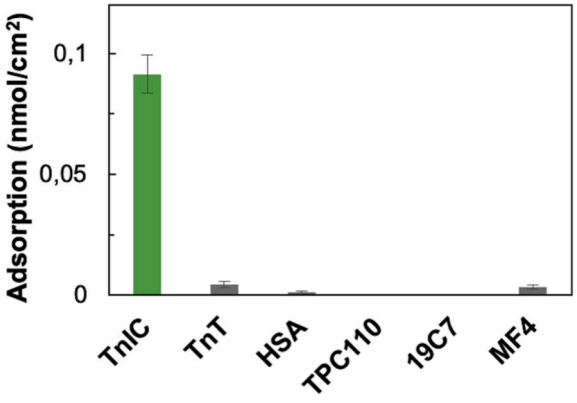

Fig. 4. Response of MIP biosensor at 20 nM of TnIC, TnT and HSA; 7 nM TPC110, 19C7 and MF4. The protein adsorption (nmol/cm^2) values are calculated from the Resonance Unit (RU), considering the different molecular weights of the analytes and that 1 RU = 0.1 ng/cm^2. The results are reported as mean value of three replicates for each analyte injections. Each injection was followed by a regeneration step.

literature, concerning the detection of small molecules (e.g. alkaloids, amino acids, peptides and antibiotics), mostly in the ELISA format, where the MIP receptors showed comparable or better performances to oriented antibodies (Chianella et al., 2013; Schirhagl et al., 2010; Smolinska-Kempisty et al., 2016; Vikholm-Lundin et al., 2008). To the best of our knowledge, no comparative studies have been made between imprinted polycatecholamines and antibodies for the recognition of proteins. Here we reported preliminary data on the comparison between the PNE-based MIP biosensor and a classical oriented-antibody-based platform. In particular, the binding capacity of the MIP biosensor toward the target analyte TnIC was compared to that given by a commercial gold sensor chip with pre-immobilized streptavidin (SA), that we subsequently functionalized with a pair of biotinylated anti-TnI antibodies regularly used in commercial bioassays for TnI detection (Fig. 5). After conditioning the SA sensor chip in HBS-EP pH 7.4, three consecutive injections of 1 M NaCl in 100 mM NaOH (1 min at 5 μL min^{-1}) were performed as recommended by the manufacturer. Then, the 1:1 mixture of the biotinylated antibodies TPC110 and 19C7 (2.5 mg L^{-1} each) was injected at 5 μL min^{-1} for 4 min, showing a SPR response of 1.020 RU. A second equal injection was performed in order to ensure the saturation of the surface (ΔRU = 0). Finally, TnIC (20 nM) was injected on the functionalized biosensor (5 μL min^{-1}, 4 min), resulting in a much lower response with respect to the signal obtained with the MIP biosensor, which exhibited a higher capture capacity toward the target analyte (5.2 times higher).

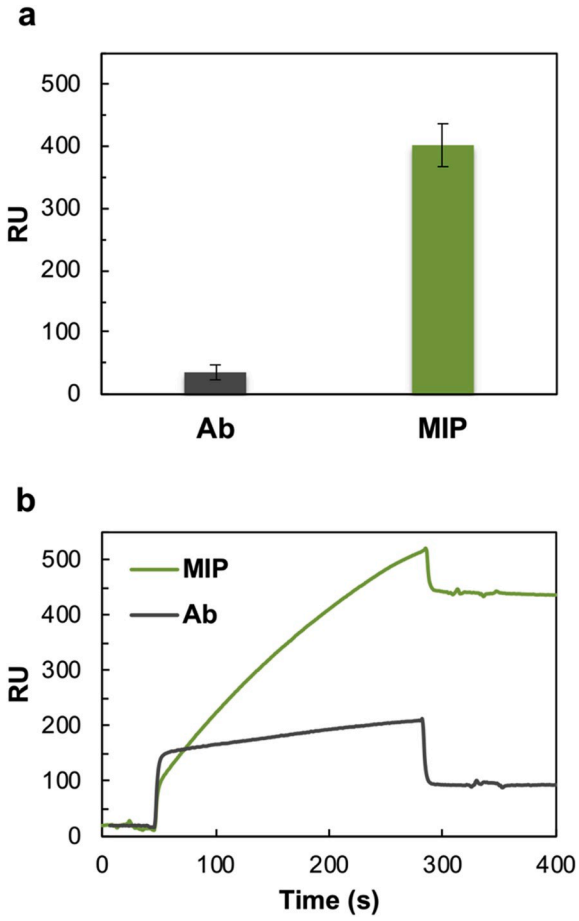

Fig. 5. (a) Response of MIP and Ab-coated biosensors at 20 nM TnIC. The control channel of the SA chip, with no antibodies, showed a TnIC response of 29 RU, that was subtracted from the graph. The results are reported as mean value of three replicates for each analyte injections. Each injection was followed by a regeneration step. (b) Representative sensorgrams about the interaction of 20 nM TnIC on the MIP (green curve) and on the Ab-coated biosensor (grey curve). (For interpretation of the references to color in this figure legend, the reader is referred to the Web version of this article.)

3.6. Kinetic analysis and calibration curves

The binding affinity between TnIC and the MIP surface was assessed by SPR measurements, following a Single-Cycle Kinetic set-up (SCK). In SCK, a series of increasing concentrations of the analyte is sequentially injected, without regeneration steps between each injection. TnIC was injected at 5 μL^{-1} flow rate at the following concentrations: 2.5, 5, 10, 15 and 20 nM. The kinetic parameters were then analyzed with the BiaEvaluation software, by following the Langmuir 1:1 binding model, which assumes a simple reversible bimolecular interaction between the analyte and the ligand (Fig. 6a). As result, a K_D value of 4.4 nM was found by fitting the model with the SPR response, confirming the impressive affinity between MIP cavities and TnIC. Furthermore, the same kinetic study was also performed on the correspondent MIP PDA-based biosensor, in order to compare the affinity of the analyte toward both the polymers (data not showed). As result, the PDA biosensor presented a good linearity until 10 nM, while for lower concentrations the sensitivity decreases. The estimated K_D was found to be around 960 nM, confirming the better affinity of PNE respect to PDA for the selected analyte. The sensitivity of the MIP sensor chip toward the analyte TnIC was firstly assessed in PBS pH 7.4 by measuring the SPR response to different concentrations of TnIC in the low nanomolar range. Each injection was followed by a regeneration step. Fig. 6b (orange) shows that the imprinted biosensor linearly responds to increasing concentrations of TnIC, resulting in a limit of detection of 460 ± 56 pM. Even if the use of PNE-based MIP allows to limit the non-specific adsorption on separated plasma components in a satisfactory extent (Fig. 4), we further decided to introduce and optimize the pre-analytical extraction of TnIC from plasma samples. This step was performed through the use of magnetic microbeads, as described in Paragraph 2.5. Briefly, commercial streptavidin-coated magnetic microbeads were functionalized with a biotinylated anti-TnI antibody (MF4 clone) then, after their incubation with the spiked plasma samples, TnIC was eluted at acidic pH, neutralized and injected in the SPR platform. The detection of TnIC in human plasma (HS) spiked with TnIC at the same concentrations tested in buffer is reported in Fig. 6c (orange). As result, the biosensor linearly responds to the increasing concentrations of the analyte up to 20 nM range, showing a sensibly lower slope and thus a higher detection limit, estimated to be 8.9 ± 1.9 nM in a direct assay design. The LOD obtained by the direct detection of the analyte on the MIP, however, is far from the clinical performance requested by the international guidelines, ca. 40 ng/L (0.45 pM) within the first 6 h from the onset of symptoms.

Therefore, we extended the development of the assay by introducing a monoclonal antibody directed to TnC. The rationale behind this choice arises from the fact that the MIP imprinting was designed against the N-terminus of TnI monomer. Therefore, we assume that an anti-TnI antibody as secondary recognition element could be impaired by the limited exposition of this subunit towards the bulk. On the contrary, we may suppose that the TnC subunit, not directly involved into the direct binding with the MIP surface, could be more suitably available for any kind of further signal amplification architecture. To this aim, we selected the alkaline phosphatase-labeled anti-TnC antibody (LS-C511913) to obtain a sandwich-like detection strategy. The presence of alkaline phosphatase will allow in the near future to exploit the MIP here developed on high-sensitivity colorimetric/fluorimetric platforms, i.e. in ELISA-type format, taking advantage of enzyme amplification. To demonstrate the feasibility of the idea, the anti-TnC antibody was injected on the TnIC already captured on the MIP surface, at increasing concentrations in the low nanomolar range. Each injection was followed by the addition of the antibody at 10 mg L^{-1} and then by a regeneration step. The strategy allowed, *per se*, to lower the detection limit of the assay in buffer solution (193 ± 30 pM), thanks to the mass enhancement evoked by the antibody. The calibration showed an excellent correlation

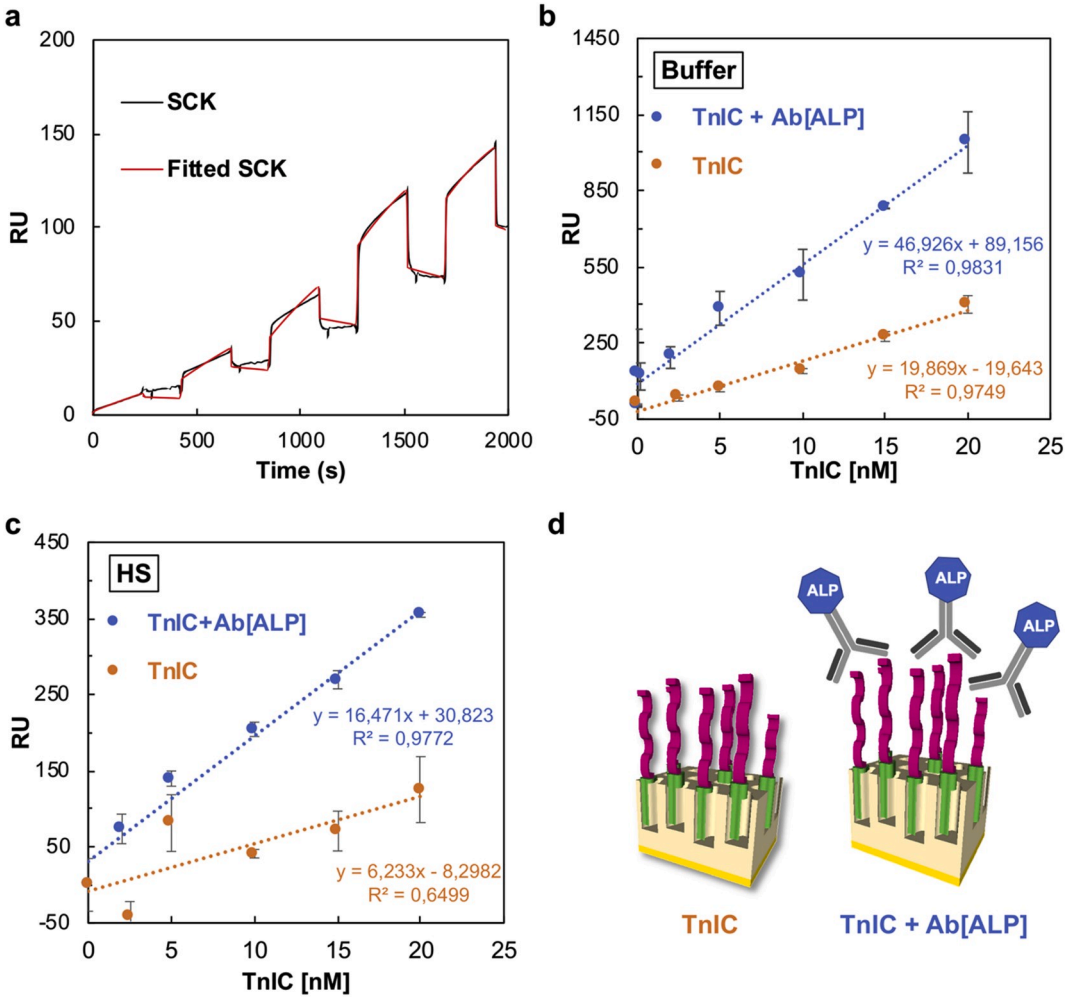

Fig. 6. (a) Sensorgram (black curve) of the SCK run by injecting five increasing concentrations of TnIC (2.5, 5, 10, 15 and 20 nM) on the MIP biosensor. The red curve represents the best fit of the sensorgram with the 1:1 binding model. (b) Linear fitting of MIP response to different concentrations of TnIC in PBS pH 7.4 followed by injections of alkaline phosphatase-labeled anti-TnC antibody (blue), compared to the not amplified response (orange). (c) Linear fitting of MIP response to different concentrations of TnIC in human serum (HS) followed by injections of alkaline phosphatase-labeled anti-TnC antibody (blue), compared to the not amplified response (orange). (For interpretation of the references to color in this figure legend, the reader is referred to the Web version of this article.)

coefficient ($R^2 = 0.98$).

The approach applied to spiked HS allowed to considerably improve both the linearity and the reproducibility (Fig. 6c), even if the LOD was maintained in the low nanomolar range (7.1 ± 0.6 nM).

As a whole, the protocol allowed the direct detection of TnIC with excellent binding affinity and good selectivity in complex real matrix but needs further work to gain the detection limit in human matrix, e.g. fluorescence-based instrumentation.

4. Conclusions

Here it is presented the first example on the use of NE as functional monomer for imprinted optical biosensors and its applicative study on the detection of TnI, a crucial biomarker for acute cardiac failures (Wettersten and Maisel, 2015; Zahran et al., 2018). The almost totally absent interest in PNE-based sensors, in contrast with the impressive interest expressed for PDA by the scientific community (2 and 329 documents in the last 10 years, respectively, source Scopus.com) caught our attention (Palladino et al., 2019; Zaidi, 2017). In particular, we wondered why this significant gap, despite such a small structural difference between these two biopolymers. Could the additional hydroxyl group of NE open new perspectives in the field of molecular imprinting? Thus, we were encouraged to investigate the use of NE for the synthesis of molecularly imprinted polymers, looking for additional properties that could justify its inclusion in the list of successful functional monomers for biosensing applications and, in particular, protein detection. In this work, we showed how the increased hydrophilicity of PNE surfaces can reduce the non-specific adsorption of proteins, driven by the hydrophobic interactions with the surface, by bringing advantages in terms of the MIP biosensor selectivity. As a case study, a PNE-based MIP biosensor for TnI coupled with SPR transduction was successfully prepared, showing a) excellent selectivity for the target protein; b) higher capture capacity, respect to a correspondent antibody-based biosensor; c) excellent kinetic binding constant in the very low nanomolar range promising results in human matrix. However, an issue on its sensitivity remains, and we here report an amplification strategy based on anti-TnC antibody labeled with alkaline phosphatase for the perspective application of the MIP developed on high-sensitivity colorimetric/fluorimetric platforms, i.e. in ELISA-type format, taking advantage of enzyme amplification.

Declaration of competing interest

The authors declare that they have no known competing financial interests or personal relationships that could have appeared to influence the work reported in this paper.

CRediT authorship contribution statement

V. Baldoneschi: Conceptualization, Methodology, Investigation, Writing - original draft, Writing - review & editing. **P. Palladino:** Investigation, Data curation, Writing - review & editing. **M. Banchini:** Software, Investigation. **M. Minunni:** Writing - review & editing, Supervision. **S. Scarano:** Conceptualization, Methodology, Investigation, Writing - review & editing, Supervision, Project administration, Funding acquisition.

Acknowledgements

The authors thank the Italian Ministry of Education, University and Research (MIUR) for financial support through the Project "Dipartimenti di Eccellenza 2018-2022" allocated to the Department of Chemistry "Ugo Schiff", and the Italian Ministry of Health (Section for the supervision and control of doping and for the protection of health in sports activities of the Technical Health Committee) for the financial support within the call "Research and training/information program on drugs, medical substances and practices that can be used for doping purposes and for health protection in sporting activities" (cooperation agreement n. 2018-4).

References

Accardo, A., Morisco, A., Palladino, P., Palumbo, R., Tesauro, D., Morelli, G., 2011. Amphiphilic CCK peptides assembled in supramolecular aggregates: structural investigations and in vitro studies. Mol. Biosyst. 7, 862–870.

Ansari, S., Masoum, S., 2019. Molecularly imprinted polymers for capturing and sensing proteins: current progress and future implications. Trends Anal. Chem. 114, 29–47.

Baldoneschi, V., Palladino, P., Scarano, S., Minunni, M., 2020. Polynorepinephrine: state-of-the-art and perspective applications in biosensing and molecular recognition. Anal. Bioanal. Chem. https://doi.org/10.1007/s00216-020-02578-9. Available online 20 March 2020, 112161, In press.

Blows, W.T., 2000. Neurotrasmitters of the brain: serotonin noradrenaline (norepinephrine), and dopamine. J. Neurosci. Nurs. 32, 234–238.

Buchwalow, I., Samoilova, V., Boecker, W., Tiemann, M., 2011. Non-specific binding of antibodies in immunohistochemistry: fallacies and facts. Sci. Rep. 1, 1–6.

Casadio, S., Lowdon, J.W., Betlem, K., Tadashi, J., Foster, C.W., Cleij, T.J., van Grinvsen, B., Sutcliffe, O.B., Banks, C.E., Peeters, M., 2017. Development of a novel flexible polymer-based biosensor platform for the thermal detection of noradrenaline in aqueous solutions. Chem. Eng. J. 315, 459–468.

Chen, J., Liang, R.P., Wang, X.N., Qiu, J.D., 2015. A norepinephrine coated magnetic molecularly imprinted polymer for simultaneous multiple chiral recognition. J. Chromatogr. A 1409, 268–276.

Chianella, I., Guerriero, A., Moczko, E., Caygill, J.S., Piletska, E.V., Perez De Vargas Sansalvador, I.M., Whitcombe, M.J., 2013. Direct replacement of antibodies with molecularly imprinted polymer (MIP) nanoparticles in ELISA - development of a novel assay for vancomycin. Anal. Chem. 85, 8462–8468.

D'Agata, R., Palladino, P., Spoto, G., 2017. Streptavidin-coated gold nanoparticles: critical role of oligonucleotides on stability and fractal aggregation. Beilstein J. Nanotechnol. 8, 1–11.

Giuliani, I., Bertinchant, J., Granier, C., Laprade, M., Chocron, S., Toubin, G., Etievent, J., Larue, C., Trinquier, S., 1999. Determination of cardiac troponin I forms in the blood of patients with acute myocardial infarction and patients receiving crystalloid or cold blood cardioplegia. Clin. Chem. 45, 213–222.

Goh, S.C., Luan, Y., Wang, X., Du, H., Chau, C., Schellhon, H.E., Brash, J.L., Chen, H., Fang, Q., 2018. Polydopamine-polyethylene glycol-albumin antifouling coatings on multiple substrates. J. Mater. Chem. B 6, 940–949.

He, Z., Su, H., Shen, Y., Shi, W., Liu, X., Liu, Y., Zhang, F., Zhang, Y., Sun, Y., Ge, D., 2019. Poly(norepinephrine)-coated FeOOH nanoparticles as carriers of artemisinin for cancer photothermal-chemical combination therapy. RSC Adv. 9, 9968–9982.

Hong, S., Kim, J., Na, Y.S., Park, J., Kim, S., Singha, K., Im, G.-I., Han, D., Kim, W.J., Lee, H., 2013. Poly(norepinephrine): ultrasmooth material-independent surface chemistry and nanodepot for nitric oxide. Angew. Chem. Int. Ed. 52, 9187–9191.

Huang, B., Chen, Y., Wang, G., Liu, C., 2011. Preparation and evaluation of a monolithic molecularly imprinted polymer for the chiral separation of neurotransmitters and their analogues by capillary electrochromatography. J. Chromatogr. A 1218, 849–855.

Jeon, Y.J., Kang, S.M., 2013. Chemically stable poly(norepinephrine) coatings on solid substrates by post-oxidation. Polym. Degrad. Stabil. 98, 1271–1273.

Kang, S.M., Rho, J., Choi, I.S., Messersmith, P.B., Lee, H., 2009. Norepinephrine: material-independent, multifunctional surface modification reagent. J. Am. Chem. Soc. 131, 13224–13225.

Kastritis, P.L., Bonvin, A.M.J.J., 2012. On the binding affinity of macromolecular interactions: daring to ask why proteins interact. J. R. Soc. Interface 10, 20120835.

Katrukha, A.G., Bereznikova, A.V., Esakova, T.V., Pettersson, K., Lo, T., Severina, M.E., Pulkki, K., Gusev, N.B., 1997. Troponin I is released in bloodstream of patients with acute myocardial infarction not in free form but as complex. Clin. Chem. 43, 1379–1385.

Katrukha, A.G., Bereznikova, A.V., Filatov, V.L., Esakova, T.V., Kolosova, O.V., Pettersson, K., Lovgren, T., Bulargina, T.V., Trifonov, I.R., Gratsiansky, N.A., Pulkki, K., Voipio-Pulkki, L., Gusev, N.B., 1998. Degradation of cardiac troponin I: implication for reliable immunodetection. Clin. Chem. 44, 2433–2440.

Katrukha, I.A., 2013. Human cardiac troponin complex. Structure and functions. Biochem 78, 1447–1465.

Ku, S.H., Ryu, J., Hong, S.K., Lee, H., Park, C.B., 2010. General functionalization route for cell adhesion on non-wetting surfaces. Biomaterials 31, 2535–2541.

Morjana, N.A., 1998. Degradation of human cardiac troponin I after myocardial infarction. Biotechnol. Appl. Biochem. 28, 105–111.

Nejad, M.A.F., Ghasemi, F., Hormozi-nezhad, M.R., 2018. A wide-color-varying ratiometric nanoprobe for detection of norepinephrine in urine samples. Anal. Chim. Acta 1039, 124–131.

Palladino, P., Aura, A.M., Spoto, G., 2016. Surface plasmon resonance for the label-free detection of Alzheimer's β-amyloid peptide aggregation. Anal. Bioanal. Chem. 408, 849–854.

Palladino, P., Bettazzi, F., Scarano, S., 2019. Polydopamine: surface coating, molecular imprinting, and electrochemistry — successful applications and future perspectives in (bio)analysis. Anal. Bioanal. Chem. 411, 4327–4338.

Palladino, P., Minunni, M., Scarano, S., 2018. Cardiac Troponin T capture and detection in real-time via epitope-imprinted polymer and optical biosensing. Biosens. Bioelectron. 106, 93–98.

Palladino, P., Portella, L., Colonna, G., Raucci, R., Saviano, G., Rossi, F., Napolitano, M., Scala, S., Castello, G., Costantini, S., 2012. The N-terminal Region of CXCL11 as structural template for CXCR3 molecular recognition: synthesis, conformational analysis, and binding studies. Chem. Biol. Drug Des. 80, 254–265.

Palladino, P., Scaglione, G.L., Arcovito, A., Vitale, M.R., Amodeo, P., Vallone, B., Brunori, M., Benedetti, E., Rossi, F., 2011. Neuroglobin-prion protein interaction: what's the function? J. Pept. Sci. 17, 387–391.

Park, K.C., Gaze, D.C., Collinson, P.O., Marber, M.S., 2017. Cardiac troponins: from myocardial infarction to chronic disease. Cardiovasc. Res. 113, 1708–1718.

Peters, T.J., 1996. All about Albumin. Biochemistry, Genetics, and Medical Applications. Academic Press, San Diego.

Pop-Georgievski, O., Popelka, S., Houska, M., Proks, V., Rypacek, F., 2011. Poly(ethylene oxide) layers grafted to dopamine-melanin anchoring layer: stability and resistance to protein adsorption. Biomacromolecules 12, 3232–3242.

Rosy, Chasta, H., Goyal, R.N., 2014. Molecularly imprinted sensor based on o-aminophenol for the selective determination of norepinephrine in pharmaceutical and biological samples. Talanta 125, 167–173.

Scarano, S., Palladino, P., Pascale, E., Brittoli, A., Minunni, M., 2019. Colorimetric determination of p-nitrophenol by using ELISA microwells modified with an adhesive polydopamine nanofilm containing catalytically active gold nanoparticles. Microchim. Acta 186, 146.

Scarano, S., Pascale, E., Palladino, P., Fratini, E., Minunni, M., 2018. Determination of fermentable sugars in beer wort by gold nanoparticles@polydopamine: a layer-by-layer approach for localized surface plasmon resonance measurements at fixed wavelength. Talanta 183, 24–32.

Schirhagl, R., Podlipna, D., Lieberzeit, P.A., Dickert, F.L., 2010. Comparing biomimetic and biological receptors for insulin sensing. Chem. Commun. 46, 3128–3130.

Singh, M., Gupta, N., Raghuwanshi, R., 2017. Epitope imprinting approach to monitor diseases. J. Mol. Genet. Med. 11, 1000270.

Smolinska-Kempitsty, K., Guerriero, A., Canfarotta, F., Càceres, C., Whitcombe, M.J., Piletsky, S., 2016. A comparison of the performance of molecularly imprinted polymer nanoparticles for small molecule targets and antibodies in the ELISA format. Sci. Rep. 6, 37638.

Sy, K.H.S., Ho, L.W.C., Lau, W.C.Y., Ko, H., Choi, C.H.J., 2018. Morphological diversity, protein adsorption, and cellular uptake of polydopamine-coated gold nanoparticles. Langmuir 34, 14033–14045.

Takeda, S., Yamashita, A., Maeda, K., Mae, Y., 2003. Structure of the core domain of human cardiac troponin in the Ca2+-saturated form. Nature 424, 35–41.

Torrini, F., Palladino, P., Brittoli, A., Baldoneschi, V., Minunni, M., Scarano, S., 2019. Characterization of troponin T binding aptamers for an innovative enzyme-linked oligonucleotide assay (ELONA). Anal. Bioanal. Chem. 411, 7709–7716.

Uzun, L., Turner, A.P.F., 2016. Molecularly-imprinted polymer sensors: realising their potential. Biosens. Bioelectron. 76, 131–144.

Vikholm-Lundin, I., Pulli, T., Albers, W.M., Tappura, K., 2008. A comparative evaluation of molecular recognition by monolayers composed of synthetic receptors or oriented antibodies. Biosens. Bioelectron. 24, 1036–1038.

Wei, F., Wu, Y., Xu, G., Gao, Y., Yang, J., Liu, L., Zhou, P., Hu, Q., 2014. Molecularly imprinted polymer based on CdTe@SiO2 quantum dots as a fluorescent sensor for the recognition of norepinephrine. Analyst 139, 5785–5792.

Wettersten, N., Maisel, A., 2015. Role of cardiac troponin levels in acute heart failure. Card. Fail. Rev. 1, 102–106.

Yang, D., Wang, X., Ai, Q., Shi, J., Jiang, Z., 2015. Performance comparison of immobilized enzyme on the titanate nanotube surfaces modified by poly(dopamine) and poly(norepinephrine). RSC Adv. 5, 42461–42467.

Zahran, S., Figueiredo, V.P., Graham, M.M., Schulz, R., Hwang, P.M., 2018. Proteolytic digestion of serum cardiac troponin I as marker of ischemic severity, 3, 450–455. Focus. Reports.

Zaidi, S.A., 2019. An account on the versatility of dopamine as a functional monomer in molecular imprinting. ChemistrySelect 4, 5081–5090.
Zaidi, S.A., 2017. Molecular imprinting polymers and their composites: a promising material for diverse applications. Biomater. Sci. 5, 388–402.
Zhang, Y.Z., Zhang, J.W., Wang, C.Z., Zhou, L. Di, Zhang, Q.H., Yuan, C.S., 2018. Polydopamine-coated magnetic molecularly imprinted polymers with fragment template for identification of pulsatilla saponin metabolites in rat feces with UPLC-Q-TOF-MS. J. Agric. Food Chem. 66, 653–660.